Wind and Structures, *Vol. 30, No. 3 (2020) 289-298*
DOI: https://doi.org/10.12989/was.2020.30.3.289

Prediction of downburst-induced wind pressure coefficients on high-rise building surfaces using BP neural network

Zhiyuan Fang, Zhisong Wang* and Zhengliang Li

School of Civil Engineering, Chongqing University, Chongqing 400045, China

(Received June 18, 2019, Revised July 24, 2019, Accepted December 10, 2019)

Abstract. Gusts generated by downburst have caused a great variety of structural damages in many regions around the world. It is of great significance to accurately evaluate the downburst-induced wind load on high-rise building for the wind resistance design. The main objective of this paper is to propose a computational modeling approach which can satisfactorily predict the mean and fluctuating wind pressure coefficients induced by downburst on high-rise building surfaces. In this study, using an impinging jet to simulate downburst-like wind, and simultaneous pressure measurements are obtained on a high-rise building model at different radial locations. The model test data are used as the database for developing back propagation neural network (BPNN) models. Comparisons between the BPNN prediction results and those from impinging jet test demonstrate that the BPNN-based method can satisfactorily and efficiently predict the downburst-induced wind pressure coefficients on single and overall surfaces of high-rise building at various radial locations.

Keywords: downburst; pressure coefficient; high-rise building; impinging jet; BP neural network

1. Introduction

For structural wind engineering, previous studies mainly focused on atmospheric boundary layer wind. However, A large number of wind disasters show that extreme wind is the main cause of structural damage (Letchford *et al*. 2002, Yang *et al*. 2018). Studies have shown that in many non-typhoon areas, downburst is the primary source of extreme wind and responsible for the design wind speed (Chay and Letchford 2002). The downburst is the local strong wind event that frequently occurs during the thunderstorm weather. Fujita (1985) defined it as “a strong downdraft which induces an outburst of damaging winds on or near the ground”. Due to the different formation mechanisms, the wind field characteristics of the downburst are quite different from those of the atmospheric boundary layer (ABL). The typical velocity profile of downburst is nose-shaped, and it would lead to a higher near-ground wind speed than that in ABL (e.g., Peng *et al*. 2018). The corresponding wind load and its potential tremendous damage to structures have attracted more and more attention (e.g., Holmes and Oliver 2000, Damatty and Huang 2018).

Compared with most engineering structures, high-rise building is more sensitive to wind loads due to their light weight, large flexibility, low damping ratio, and low fundamental frequencies. In addition, the glass curtain wall used in high-rise building is also facing the threat of extreme winds. Neglecting or incorrectly predicting the wind loads of high-rise buildings under extreme winds will result in huge hidden dangers to the structural safety and will greatly increase the maintenance cost of the envelope structure. Therefore, it is of great significance to study the characteristics of downburst-induced wind loads on high-rise buildings.

At present, there are mainly two ways to study wind loads. The first method is to conduct wind tunnel tests, and it is considered to be the accurate method to study the wind pressure on surfaces of a building. However, it is expensive and difficult to take into account all possible wind load conditions. Furthermore, if building shape is complex, it will be hard to avoid arranging too many pressure taps with the purpose of obtaining the detailed wind load characteristics. In addition, most of the existing wind tunnels are mainly used to simulate atmospheric boundary layer wind, and only a few wind tunnels have the conditions for downburst test, which also brings some obstacles to downburst experimental research. Another method is numerical simulation, which is based on Computational Fluid Dynamics (CFD). With the development of computer technology, numerical simulation methods have made rapid progress in recent years. Nevertheless, its results are still greatly influenced by grid quality, boundary conditions, solving methods, and turbulence models, etc. The wind pressure distribution on the surface of the bluff body obtained by CFD is still very difficult to be highly consistent with the test results. Therefore, it is necessary to establish a computational modeling approach which can satisfactorily predict the mean and fluctuating wind pressure coefficients induced by downburst on high-rise building surfaces.

To develop a forecasting model for the problem of multiple independent variables, the multiple regression analysis is commonly used, mainly including multiple linear regression and polynomial regression. Multiple linear regression is simple and practical, but it is not well adaptive to study the complicated problem. Polynomial regression

*Corresponding author, Professor
E-mail: wangzhisong@cqu.edu.cn

http://www.techno-press.com/journals/was&subpage=7
ISSN: 1226-6116 (Print), 1598-6225 (Online)

can be used to fit non-linear problems, but it will be very difficult to solve the problem involving a large number of parameters. For the current problem, the influential parameters may include the location of the building, coordinates of pressure taps, the orientation of each surface. These factors may make the modeling process very complicated and it is hard to obtain an ideal regression equation. Artificial neural networks (ANN) developed in recent years provide us with a new choice. ANN is a computing model that simulates the structure of biological neural networks. It is a data-driven statistical method which calculated by many neuron connections. ANN can continuously adjust the internal structure based on the error between the predicted value and the target value, and finally obtains a neural network structure which can accurately predict the experimental value. This method has a strong self-adaptive ability and well robustness, which make it easy to be used to solve the complex nonlinear problems.

Since Back-propagation (BP) algorithm was developed (Rumelhart 1988), artificial neural networks have been widely used in civil engineering applications (Benardos and Kaliampakos 2004, Kim and Kim 2008, Goh and Zhang 2012, Zhang and Goh 2013, Huang, He *et al*. 2015, Kordnaeij Kalantary *et al*. 2015, Zhang and Goh 2016, Nejad and Jaksa 2017). In the field of structural wind engineering, this method has also achieved good applications, including investigation of interference effects between adjacent high-rise buildings (Khanduri, Bédard *et al*. 1997, English and Fricke 1999), prediction of wind pressure coefficients and even pressure time series on building surface (Chen, Kopp *et al*. 2003, Fu, Liang *et al*. 2007, Chen, Wu *et al*. 2008, Huang He *et al*. 2017, Bre, Gimenez *et al*. 2018). These studies have successfully applied the ANN method to the engineering field and achieved good results. But as far as I know, the ANN method has not been applied in the field of downburst wind load so far.

Downburst-modeling methods mainly include impinging jet modeling, wall jet modeling and ring-vortex modeling, etc. Among them, the impinging jet model has been widely used by many scientific researchers (Holmes and Oliver 2000, Choi 2004, Mason Letchford *et al*. 2005) due to its simplicity and ability to simulate downburst wind field reasonably. In this paper, using the experimental equipment based on the impinging-jet-model, the pressure test of the high-rise building model at different locations was conducted in the laboratory, and the measured pressure data was used as the database to develop artificial neural networks models. The Back propagation neural network (BPNN) method was used to modeling the mean and fluctuating wind pressure coefficients of the building surfaces, and the prediction accuracy of models were quantitatively analysed.

2. Wind tunnel experiments

2.1 Experimental setup

Experiments were conducted by using the impinging-jet-based downburst generator at Zhejiang University, China. The test facility is mainly composed of jet nozzle, flat plate and measurement system. As shown in Fig. 1, the distance between flat plate and jet nozzle is 1.2 m (i.e., H_{jet}=1.2 m). The diameter of jet nozzle is 0.6 m (i.e., D_{jet}=0.6 m). The velocity at the nozzle exit was set to 12 m/s (i.e., V_{jet}=12 m/s).

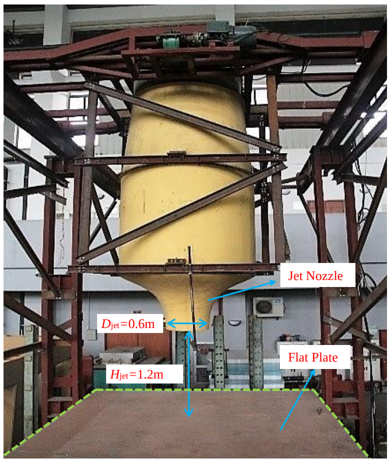

Fig. 1 The photo of test facility

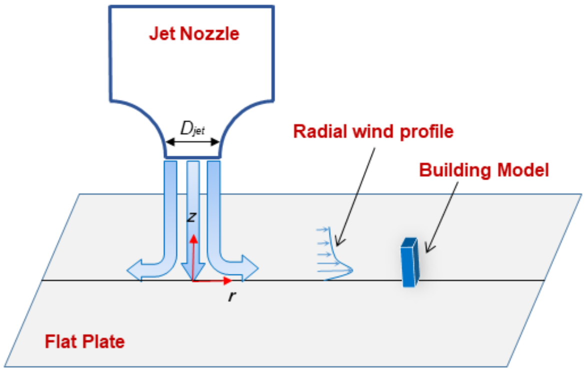

(a)

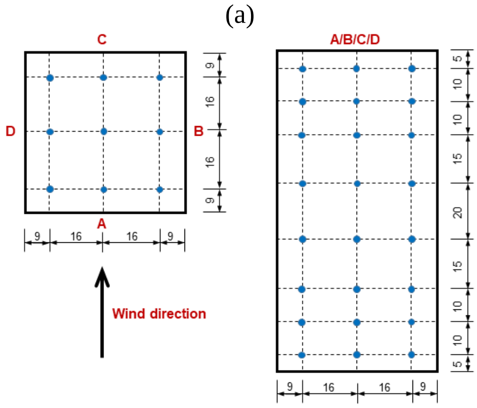

(b)

Fig. 2 Schematic arrangements of measuring pressure test of high-rise building model

Fig. 2 shows the schematic of the flow circuit and high-rise building model used in current study. As shown in Fig. 2(a), the jet nozzle generate a downdraft flow which impacts on the flat plate and spread from center to periphery. With the increase of airflow spread distance, the

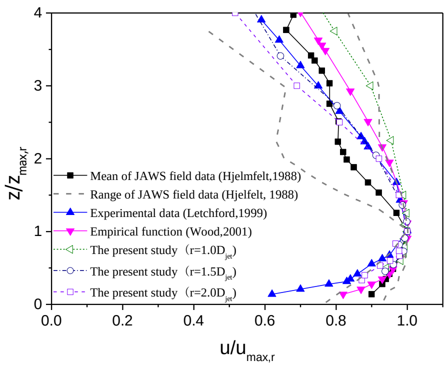

Fig. 3 Comparison of measured radial wind profile with published data

characteristics of near-surface wind field will change significantly, which will affect the wind pressure distribution on the surface of high-rise building model. Therefore, the radial distance from the building model to the center of the downdraft flow (r) is taken into account as an important influence parameter. In this study, the high-rise building model was measured at r/D_{jet}=1.0, 1.25, 1.5, 1.75, 2.0, 2.25, 2.5 and 3.0. The geometric scale ratio of test is 1:1000, so the model with the dimension of 50 mm× 50 mm× 100 mm would represent high-rise building with 50 m× 50 m in plan and 100 m in height, and the corresponding actual diameter of downburst is 600 m. As shown in Fig. 2(b), the windward surface is marked as face-A, the leeward surface as face-C, two side surface as face-B and face-D respectively, and the roof surface as face-S. Each of the face A/B/C/D was equipped with 24 pressure taps, and face S was equipped with 9 pressure taps. During the test, the sampling frequency of the measuring data is 312.5 Hz and the sampling time is 32s.

2.2 Wind flow characteristics

In the present study, the wind field characteristics were measured at eight radial locations (i.e., r/D_{jet}= 0.6, 0.8, 1.0, 1.25, 1.5, 2.0, 2.5, 3.0) by using a hot wire probe within a height range of 0~180 mm upon the ground. Fig. 3 shows the quantitative comparisons of the measured u velocity (normalized by the maximum radial velocity, $u_{max,r}$, and plotted aginst a vertical position ordinate normalized by the height where the maximum radial velocity occurred, $z_{max,r}$) at three typical radial locations (r=1.0, 1.5, 2.0D_{jet}) of the present study with JAWS field measurement data (Hjelmfelt 1988) and other previous published studies (Letchford 1999, Wood *et al.* 2001). As shown in Fig. 3, even though the details of flow features vary from case to case, their overall trend are similar, and the velocity profiles in present study are in good agreement with the JAWS field data and previous published data.

Fig. 4 gives the measured radial wind velocity as well as turbulence intensity profiles at eight radial locations, as mentioned above. It can be seen clearly that the velocity and turbulence intensity has changed a lot with the increasing of radial distance from the center of the downdraft. As shown in Fig. 4(a), the maximum radial velocity occurred at r=1.0~1.25D_{jet}, and radial velocity and

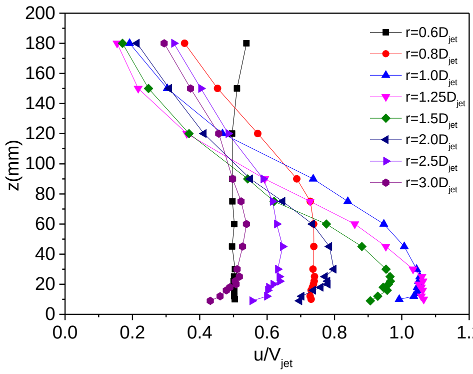

(a) radial velocity profiles

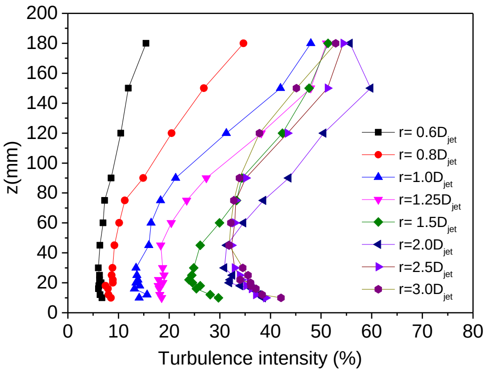

(b) turbulence intensity profiles

Fig. 4 Measured mean velocity and turbulence intensity profiles at eight typical radial locations

turbulence intensity at r<1.0D_{jet} are relatively small. So, in present study, only r>1.0D_{jet} are taken into account for the pressure test of high-rise building model.

2.3 Pressure data analysis

Wind pressure coefficients are used to describe the wind pressure characteristics of building surface, and which is generally defined as

$$C_p = \frac{p - p_{ref}}{0.5\rho V^2} \tag{1}$$

Where p is the absolute pressure, p_{ref} is a reference pressure, ρ is the air d ensity, and V is the reference wind speed utilized to compute a reference dynamic pressure for normalization. For the downburst, the velocity at nozzle exit ($V_{\rm jet}$) is generally used as V.

Figs. 5 and 6 show the mean and RMS wind pressure coefficients of the building surfaces respectively. It can be found obviously, corresponding to the wind field characteristics shown in Fig.4, the mean and RMS pressure coefficients distributed regularly with the increase of radical distance (r). The mean wind pressure coefficients on building surfaces is larger at r=1.0$D_{\rm jet}$, while the fluctuating wind pressure coefficients is larger at r=2.0$D_{\rm jet}$. Thus, as for the downburst wind field, the pressure coefficients were significantly affected by the radial distance from the high-rise building to the center of downdraft.

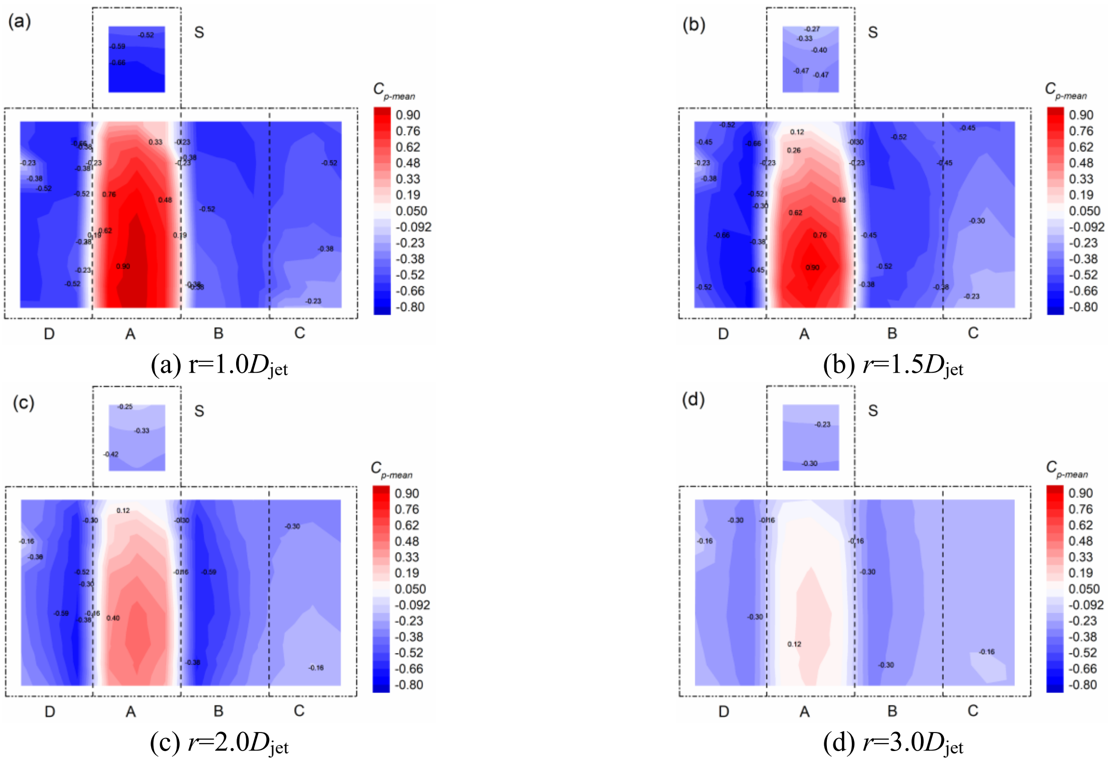

(a) r=1.0D_{jet} (b) r=1.5D_{jet}

(c) r=2.0D_{jet} (d) r=3.0D_{jet}

Fig. 5 Contours of measured Cp-mean on model surfaces at four typical radical locations

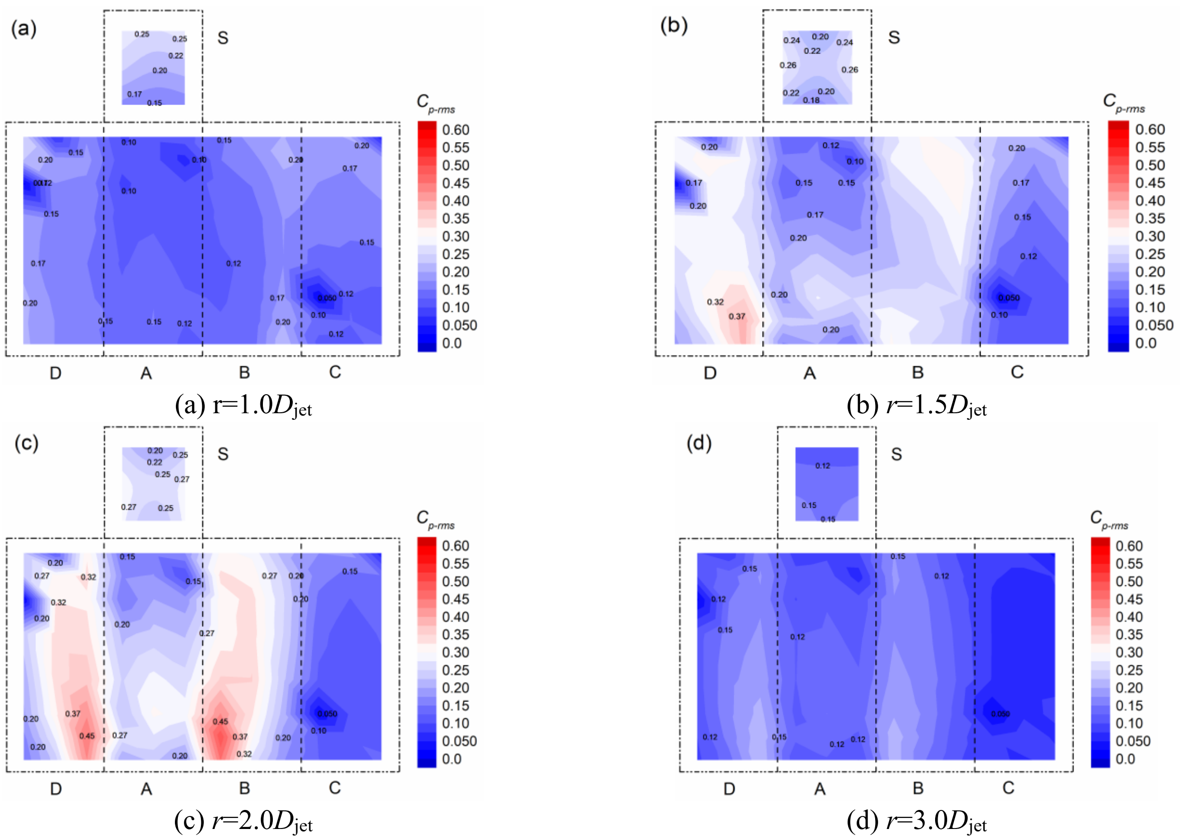

(a) r=1.0D_{jet} (b) r=1.5D_{jet}

(c) r=2.0D_{jet} (d) r=3.0D_{jet}

Fig. 6 Contours of measured Cp-rms on model surfaces at four typical radical locations

3. Back propagation neural network

Artificial neural network can be roughly divided into supervised learning network and unsupervised learning network according to learning strategies. In the process of supervised learning, the training data is added to the input

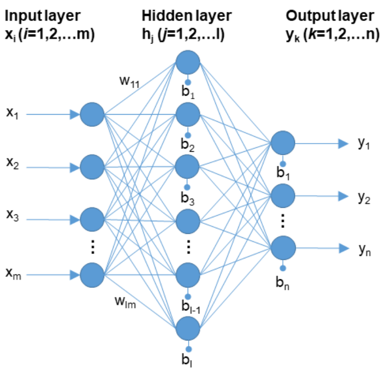

Fig. 7 Structure of Back-propagation neural network used in this study (BPNN m-l-n)

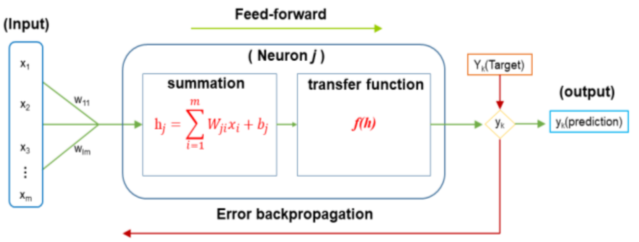

Fig. 8 Structure of Back-propagation neural network used in this study

of the neural network, and the corresponding expected output is compared with the network output to get the error signal. The connection strength of the weight value is adjusted by the error signal. After many trainings, it converges to a certain weight value. And once the sample changes, the weights will be automatically modified to adapt to the new situation. In unsupervised learning, the network is directly placed in the environment without a standard sample in advance, and the learning phase and the working phase are integrated. At this moment, the change of learning law obeys the evolution equation of connecting weights. The main purpose of this paper is to establish a mathematical model which can accurately predict the wind pressure on the surface of high-rise building under downburst by using the neural network method based on the existing experimental data, so supervised learning is more suitable for this study. In supervised learning, the BPNN model is most widely used, and its strong self-adaptive ability enables it to perform non-linear fitting, optimization, and nonlinear mapping. Based on the above points, in this paper, a neural network based on backpropagation algorithm is used to establish a three-layer feedforward neural network model for predicting the surface pressure coefficients of high-rise building due to the downburst wind. The topology structure is shown in Fig.7. The symbol BPNN *m-l-n* is used as a label for the network, which contains *m* input variables, *l* hidden neurons and *n* output variables.

The training process of backpropagation algorithm can be divided into two phases, including feed-forward as well as error back propagation. As shown in Fig. 8, in the first phase, the input of neurons J in the hidden layer is the sum of weighted inputs and bias. Then, the summation is

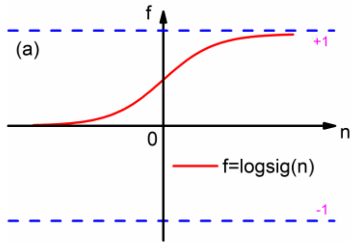

(a) f=logsig(n)

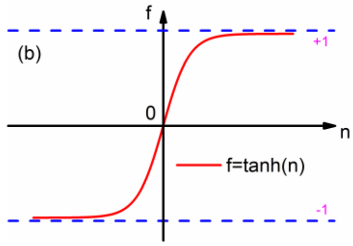

(b) f=tanh(n)

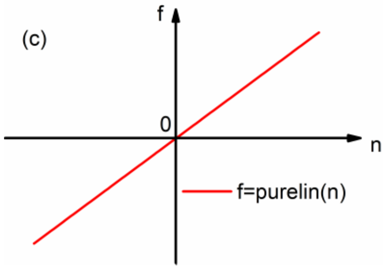

(c) f=purelin(n)

Fig. 9 Transfer function

transformed by the non-linear transfer function f (·) to generate the output signal of the neuron j, which can be expressed as

$$y_j = f\left(\sum_{i=1}^{m} W_{ji}x_i + b_j\right) \tag{2}$$

where W_{ji} is the weight which connects the *i*th neuron to the *j*th neuron); *xi* denotes the *i*th input variable; *bj* is the bias that associated with the *j*th neuron; $f(\cdot)$ means the transfer function, and it most frequently used in BPNN mainly include three types: linear function, logarithmic function, and hyperbolic tangent function. The graph of common expressions of these three type transfer functions are presented as Fig. 9.

After the first phase, the output values y_k obtained from the forward process should be compared with the target values Y_k, and then the errors between y_k and Y_k are backpropagated (i.e., errors are propagated from the output layer to the previous layers), and the connection weights between them are updated to reduce the errors. The error will be reduced to an acceptable range by looping the above two steps. The objective of the neural network training is to get the optimized weight and bias value that can describe the relationship between the input values and the output values, and finally achieve the satisfied prediction. The determination of the number of hidden neurons is performed by a trial and error process, and the number of the smallest neurons that can produce ideal results

Table 1 Parameters of BPNN for prediction of Cp-mean and Cp-rms

Terms	Face A/B/C/D		Face S		Overall faces	
Inputs	x,y,r		x,y,r		x,y,r,fn	
Outputs	Cp-mean	Cp-rms	Cp-mean	Cp-rms	Cp-mean	Cp-rms
BPNN structure	3-12-1	3-16-1	3-5-1	3-5-1	4-15-1	4-18-1
Transfer function	Logarithmic S type function (hidden layer): $f(s)=1/(1+e^{-s})$ Tangent S type function (output layer): $f(s)=\tanh(s)$		Logarithmic S type function (hidden layer): $f(s)=1/(1+e^{-s})$ Tangent S type function (output layer): $f(s)=\tanh(s)$		Logarithmic S type function (hidden layer): $f(s)=1/(1+e^{-s})$ Tangent S type function (output layer): $f(s)=\tanh(s)$	
No. of training data	144		54		630	
No. of testing data	48		18		210	

Table 2 Sample training and testing data sets for face-A

x(mm)	*y*(mm)	*r*(D_{jet})	$C_{p\text{-mean}}$	$C_{p\text{-rms}}$
Training data				
41	5	1	0.7661	0.1181
9	25	1.5	0.6901	0.1913
41	95	2.5	-0.0506	0.1279
9	5	2.5	0.1689	0.1468
25	40	2.5	0.2634	0.1935
9	75	2.5	0.0763	0.1215
41	85	1.25	0.115	0.0794
9	85	1.5	0.1891	0.1539
25	95	2.25	0.0263	0.1366
Testing data				
25	25	1.5	0.914	0.2775
41	25	1.5	0.762	0.2497
9	95	2.5	-0.0337	0.1095

(determination R^2 of the testing data set as judgement index) is usually selected. In this study, based on Matlab toolbox, a back-propagation algorithm with the Levenberge-Marquardt algorithm (Demuth and Beale 2009) was used for neural network modeling.

4. Prediction of pressure coefficients

4.1 Database

As mentioned above, the pressure coefficients are significant influenced by radial distance. But it worth to note that although the radial location of building has changed, the same surface maintains a similar distribution of wind pressure coefficients. Therefore, the prediction accuracy may be improved by considering the five typical faces of buildings separately (i.e., face A/B/C/D/S). At the same time, a neural network model through the database that contain the overall faces is also established.

For developing the neural network model about single face, the input variables of the database contain the positions of measuring points (i.e., x, y) and the radial distances (i.e., r). For developing the neural network model about overall faces, the input variables include the positions of the measuring points (i.e., x, y), the radial distances (i.e., r), and the face id (i.e., fn, A-1, B-2, C-3, D-4, S-5). Table 1 summarizes the network structure, transfer function, and number of training data and testing data of each neural network model developed in present study. Due to the large amount of data, it is essential to simplify the analysis process. For each type of analysis model, the corresponding data set is randomly divided into training set and testing set according to the ratio of 3:1. Table 2 lists some training data and testing data of face-A to further illustrate the data partitioning. Training data is used to train neural networks, and testing data is used to verify the reliability of trained model. Before the training process, input data should be normalize to (0-1) to improve the computational efficiency by using xnorm=2(xactual-xmin)/(xmax-xmin)-1(Goh and Zhang 2012)

4.2 Performance measures

The quality of the neural network model is mainly evaluated by the following indicators:
Coefficient of determination(R^2)

$$R^2 = 1 - \frac{\frac{1}{N}\sum_{i=1}^{N}(y_i - \bar{y})^2}{\frac{1}{N}\sum_{i=1}^{N}(Y_i - \bar{Y})^2} \tag{3}$$

Coefficient of Correlation(R)

$$R = \frac{\sum_{i=1}^{N}(y_i - \bar{y})(Y_i - \bar{Y})}{\sqrt{\sum_{i=1}^{N}(y_i - \bar{y})^2}\sqrt{\sum_{i=1}^{N}(Y_i - \bar{Y})^2}} \tag{4}$$

Mean square error (MSE)

$$MSE = \frac{1}{N}\sum_{i=1}^{N}(Y_i - y_i)^2 \tag{5}$$

in which $\bar{Y}$ is the average of the target values of Y_i; $\bar{y}$ is the average of the predicted y_i; N is the number of data points in the used set.

4.3 Prediction results

`Table 3 shows the results of various performance indicators for each developed BPNN model. For each performance parameter, the results of training data and testing data are both given. It can be seen that the R^2 (or R) of the training data are better than that of the testing data (due to the neural network model is trained based on the

Table 3 Performance measures for BPNN

Data sets		R^2		R		MSE	
		Tr.	Te.	Tr.	Te.	Tr.	Te.
A	Cp-mean	0.997	0.992	0.999	0.996	0.000245360	0.000520680
	Cp-rms	0.988	0.971	0.994	0.985	0.000033389	0.000093725
B	Cp-mean	0.993	0.991	0.997	0.995	0.000110750	0.000168180
	Cp-rms	0.995	0.986	0.997	0.993	0.000033640	0.000108970
C	Cp-mean	0.995	0.986	0.997	0.993	0.000056146	0.000154310
	Cp-rms	0.997	0.976	0.998	0.988	0.000007443	0.000005967
D	Cp-mean	0.996	0.989	0.998	0.994	0.000097565	0.000360090
	Cp-rms	0.994	0.988	0.997	0.994	0.000048006	0.000136170
S	Cp-mean	0.995	0.981	0.998	0.990	0.000083416	0.000254970
	Cp-rms	0.977	0.925	0.986	0.961	0.000068687	0.000261530
Overall faces	Cp-mean	0.991	0.985	0.995	0.992	0.001376500	0.001857100
	Cp-rms	0.949	0.934	0.974	0.967	0.000353920	0.000396400

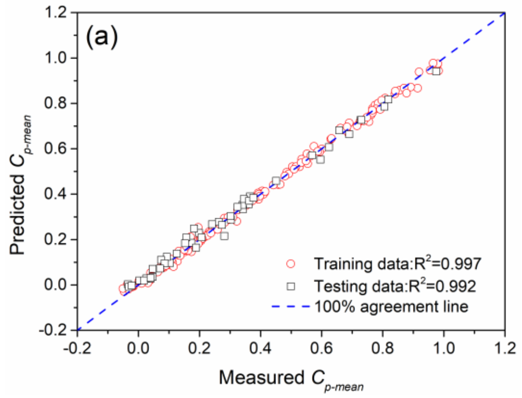

(a) face-A-Cp-mean

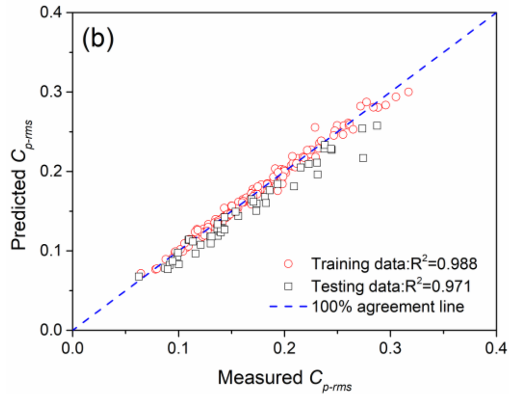

(b) face-A-Cp-rms

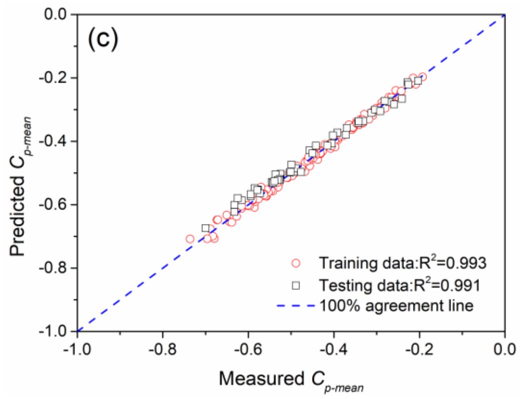

(c) face-B-Cp-mean

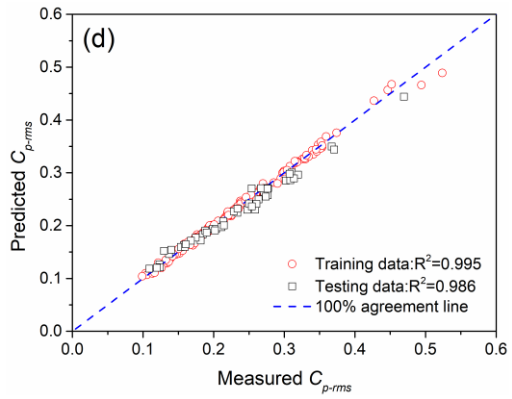

(d) face-B-Cp-rms

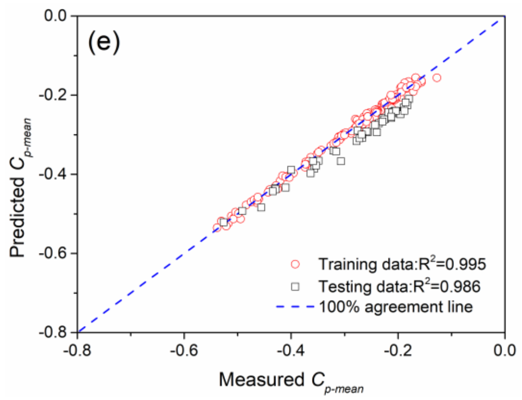

(e) face-C-Cp-mean

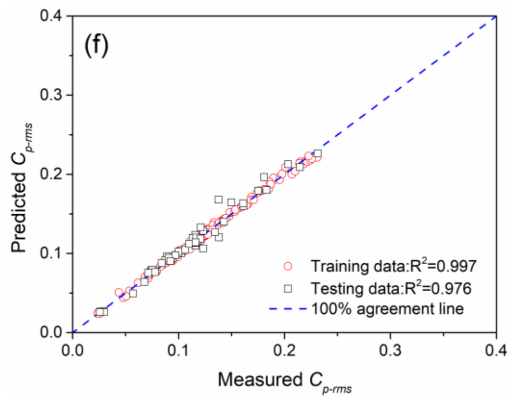

(f) face-C-Cp-rms

Fig. 10 Continued

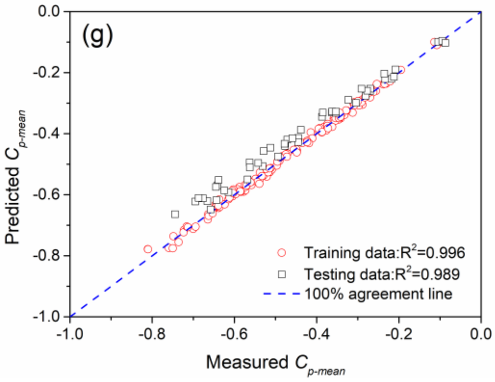

(g) face-D-Cp-mean

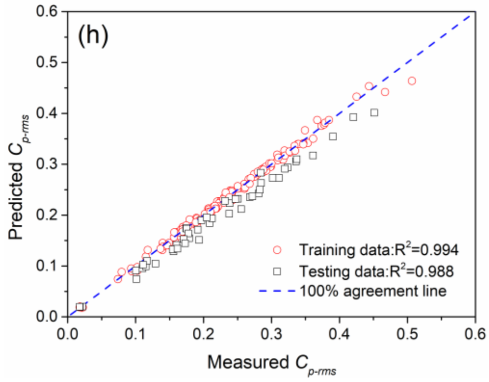

(h) face-D-Cp-rms

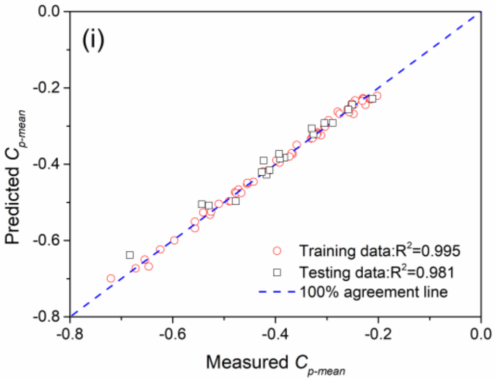

(i) face-S-Cp-mean

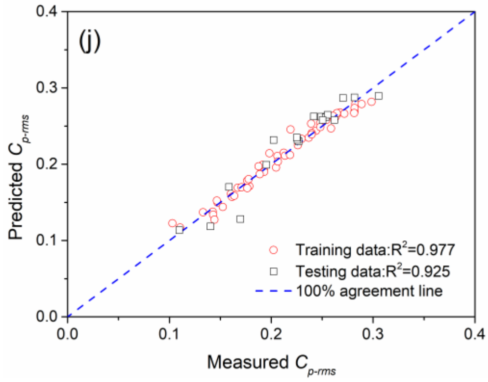

(j) face-S-Cp-rms

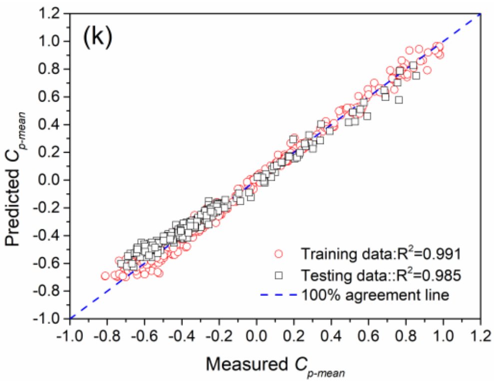

(k) face-Overall-Cp-mean

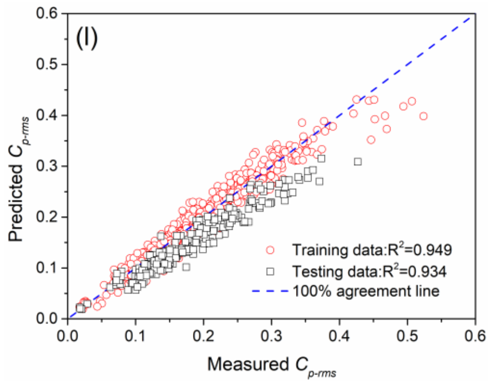

(l) face-Overall-Cp-rms

Fig. 10 Fitting between the BPNN outputs and the measured targets

training data). For the untrained testing data, the performance of the model is also ideal enough. The majority of the determination coefficient R^2 and the correlation coefficient R are above 0.98, and the minimum value is also above 0.92. The results indicate that the established neural network model can predict the measured wind pressure with high accuracy. The *MSE* reflects the degree of dispersion of the sample. It can be seen from columns 7 and 8 of Table 3 that the BPNN models developed by single face database obtain a very low *MSE* value, while the model developed by overall faces getting a slightly larger *MSE* value. It indicates that the predicted value getting from BPNN model based on single face database is more central around target value, thus it may getting a more satisfactory prediction.

Fig. 10 shows the BPNN estimations vs. the measured values for single face and overall faces models. Using the measured values as the abscissa and the predicted values as the ordinate, it can be seen clearly that the data points of the training data and testing data are basically concentrated in 100% agreement line (i.e., y=x). Both single model and overall faces models can achieve good prediction results.

In order to illustrate the prediction performance more intuitive, the contours of pressure coefficients (both Cp-mean and Cp-rms) which generated by experimental test and BPNN prediction on building surfaces at r=1.5Djet are shown in Fig.11. It can be seen that both prediction models for the single face and overall faces can satisfactorily predict the wind pressure coefficients on building surfaces. In addition, the wind pressure coefficients obtained from single face model is closer to the experimental results, and more detailed wind pressure characteristics can be captured.

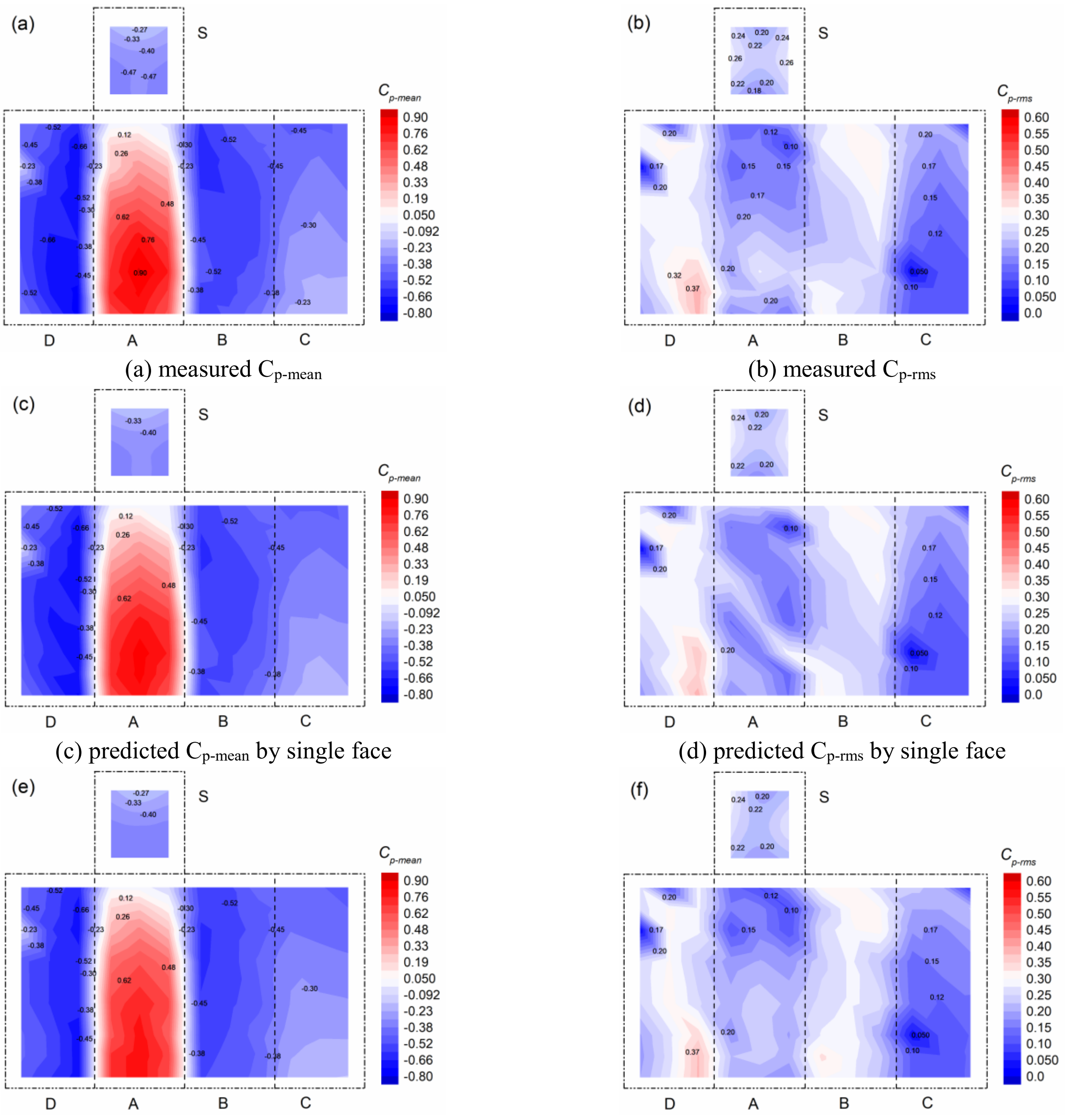

(a) measured $C_{p\text{-mean}}$ (b) measured $C_{p\text{-rms}}$

(c) predicted $C_{p\text{-mean}}$ by single face (d) predicted $C_{p\text{-rms}}$ by single face

(e) predicted $C_{p\text{-mean}}$ by overall face (f) predicted $C_{p\text{-rms}}$ by overall face

Fig. 11 Contours of pressure coefficient on model surfaces at r=1.5D_{jet}

5. Conclusions

An impinging-jet-based experimental study was conducted to assess the pressure coefficients on a high-rise building induced by the downburst-like wind. Using the back propagation neural network (BPNN) to establish prediction models for wind pressure coefficients of high-rise building under downburst. The accuracy and effectiveness of prediction models for single-face and overall-faces was validated by the comparison of the prediction results and measured data. The prediction model for single face has been proved that it could estimate the pressure coefficients more accurately and capture more detailed wind pressure characteristics. While the accuracy of prediction model for overall faces was slightly low, the process of establishing model was simpler (only one BPNN model needed to be established), and the network structure had a better generality (the model was applicable to wind pressure estimating for all surfaces). In a word, this study indicated that the back propagation neural network (BPNN) method had a good performance to predict wind pressure coefficients of high-rise building under downburst wind. This method could also be extended to the prediction of various buildings in extreme wind field.

Acknowledgments

The research reported in this paper was conducted with the support of the National Key R&D Program of China (Grant no. 2018YFC0809400) the Fundamental Research Funds for Central Universities (Grant no. CDJZR12200016) and National Natural Science Foundation of China (Grant no. 51208537). The authors are grateful to Dr. Yong Chen in Zhejiang University for his kindly helps and good suggestions during the Impinging jet experiment.

References

Benardos, A.G. and Kaliampakos, D.C. (2004), "A methodology for assessing geotechnical hazards for TBM tunnelling - illustrated by the Athens Metro, Greece", *Int. J. Rock Mech. Min*., **41**(6), 987-999. https://doi.org/10.1016/j.ijrmms.2004.03.007.

Bre, F., Gimenez, J.M. and Fachinotti, V.D. (2018), "Prediction of wind pressure coefficients on building surfaces using artificial neural networks", *Energy Build*., 158, 1429-1441. https://doi.org/10.1016/j.enbuild.2017.11.045.

Chay, M.T. and Letchford, C.W. (2002), "Pressure distributions on a cube in a simulated thunderstorm downburst - Part A: stationary downburts observations", *J. Wind Eng. Ind. Aerod*., **90**(7), 711-732. https://doi.org/10.1016/S0167-6105(02)00158-7.

Chen, C.H., Wu, J.C. and Chen, J.H. (2008), "Prediction of flutter derivatives by artificial neural networks", *J. Wind Eng. Ind. Aerod*., **96**(10-11), 1925-1937. https://doi.org/10.1016/j.jweia.2008.02.044.

Chen, Y., Kopp, G.A. and Surry, D. (2003), "Prediction of pressure coefficients on roofs of low buildings using artificial neural networks", *J. Wind Eng. Ind. Aerod*., **91**(3), 423-441. https://doi.org/10.1016/S0167-6105(02)00381-1.

Choi, E.C.C. (2004), "Field measurement and experimental study of wind speed profile during thunderstorms", *J. Wind Eng. Ind. Aerod*., **92**(3-4), 275-290. https://doi.org/10.1016/j.jweia.2003.12.001.

Damatty, A. and Huang, G. (2018), Special issue on Non-Synoptic Wind I Preface, *Wind Struct*., **26** (3), 1-1.

Demuth, H. and Beale, M. (2009). Matlab Neural Network Toolbox User's Guide Version 6, The MathWorks Inc, Natick, Massachusetts, U.S.A.

Dongmei, H., Shiqing, H., Xuhui, H., and Xue, Z. (2017), "Prediction of wind loads on high-rise building using a BP neural network combined with POD", *J. Wind Eng. Ind. Aerod*., **170**, 1-17. https://doi.org/10.1016/j.jweia.2017.07.021.

English, E.C. and Fricke, F.R. (1999), "The interference index and its prediction using a neural network analysis of wind-tunnel data", *J. Wind Eng. Ind. Aerod*., **83**(1-3), 567-575. https://doi.org/10.1016/S0167-6105(99)00102-6.

Fu, J.Y., Liang, S.G. and Li, Q.S. (2007), "Prediction of wind-induced pressures on a large gymnasium roof using artificial neural networks", *Comput. Struct*., **85**(3-4), 179-192. https://doi.org/10.1016/j.compstruc.2006.08.070.

Fujita T.T. (1985), "The Downburst", Report of Projects NIMROD and JAWS; University of Chicago, Chicago, Illinois, U.S.A

Goh, A.T.C. and Zhang, W. (2012), "Reliability assessment of stability of underground rock caverns", *Int. J. Rock Mech. Min*., **55**(10), 157-163. https://doi.org/10.1016/j.ijrmms.2012.07.012.

Hjelmfelt, M.R. (1988), "Structure and life cycle of microburst outflows observed in Colorado", *J. Appl. Meteor*, **27**(8), 900-927. https://doi.org/10.1175/1520-0450(1988)027%3C0900:SALCOM%3E2.0.CO;2.

Holmes, J.D. and Oliver, S.E. (2000), "An empirical model of a downburst", *Eng. Struct*., **22**(9), 1167-1172. https://doi.org/10.1016/S0141-0296(99)00058-9.

Huang, G., He, H., Mehta, K.C. and Liu, X. (2015), "Datab-based probabilistic damage estimation for asphalt shingle roofing", *J. Struct. Eng*., **141**(12), 04015065. https://doi.org/10.1061/(ASCE)ST.1943-541X.0001300.

Khanduri, A.C., Bédard, C. and Stathopoulos, T. (1997), "Modelling wind-induced interference effects using backpropagation neural networks", *J. Wind Eng. Ind. Aerod*., **72**(1), 71-79. https://doi.org/10.1016/S0167-6105(97)00259-6.

Kim, Y.S. and Kim, B.T. (2008), "Prediction of relative crest settlement of concrete-faced rockfill dams analyzed using an artificial neural network model", *Comput. Geotech*., **35**(3), 313-322. https://doi.org/10.1016/j.compgeo.2007.09.006.

Kordnaeij, A., Kalantary, F., Kordtabar, B. and Mola-Abasi, H. (2015), "Prediction of recompression index using GMDH-type neural network based on geotechnical soil properties", *Soils Found*., **55**(6), 1335-1345. https://doi.org/10.1016/j.sandf.2015.10.001.

Letchford, C.W. (1999), "Turbulence and topographic effects in simulated thunderstorm downdrafts by wind tunnel jet", 10th International Conference on Wind Engineering, Copenhagen, Denmark, June.

Letchford, C.W., Mans, C. and Chay, M.T. (2002), "Thunderstorms - their importance in wind engineering (a case for the next generation wind tunnel)", *J. Wind Eng. Ind. Aerod*., **90**(12), 1415-1433. https://doi.org/10.1016/S0167-6105(02)00262-3.

Mason, M.S., Letchford, C.W. and James, D.L. (2005), "Pulsed wall jet simulation of a stationary thunderstorm downburst, Part A: Physical structure and flow field characterization", *J. Wind Eng. Ind. Aerod*., **93**(7), 557-580. https://doi.org/10.1016/j.jweia.2005.05.006.

Nejad, F.P. and Jaksa, M.B. (2017), "Load-settlement behavior modeling of single piles using artificial neural networks and CPT data", *Comput. Geotech*., **89**, 9-21. https://doi.org/10.1016/j.compgeo.2017.04.003.

Peng, L., Huang, G., Chen, X. and Yang, Q. (2018), "Evolutionary spectra-based time-varying coherence function and application in structural response analysis to downburst winds", *J. Struct. Eng*., **144**(7):04018078. https://doi.org/10.1061/(ASCE)ST.1943-541X.0002066.

Rumelhart, D. (1988), Learning Internal Representation by Error Propagation, MIT Press, Cambridge, Massachusetts, U.S.A.

Wood, G.S., Kwok, K.C.S., Motteram, N.A. and Fletcher, D.F. (2001), "Physical and numerical modelling of thunderstorm downbursts", *J. Wind Eng. Ind. Aerod*., **89**(6), 535-552. https://doi.org/10.1016/S0167-6105(00)00090-8.

Yang, Q., Gao, R., Bai, F., Li, T. and Tamura, Y. (2018), "Damage to buildings and structures due to recent devastating wind hazards in East Asia", *Nat. Hazards*, **92**(3), 1-33. https://doi.org/10.1007/s11069-018-3253-8.

Zhang, W. and Goh, A.T.C. (2016), "Multivariate adaptive regression splines and neural network models for prediction of pile drivability", *Geosci. Front*, **7**(1), 45-52. https://doi.org/10.1016/j.gsf.2014.10.003.

Zhang, W.G. and Goh, A.T.C. (2013), "Multivariate adaptive regression splines for analysis of geotechnical engineering systems", *Comput. Geotech*., **48**, 82-95. https://doi.org/10.1016/j.compgeo.2012.09.016.

AD